Iranian Journal of Materials Science and Engineering, Vol. 19, Number 3, September 2022
RESEARCH PAPER

Evaluation of Microstructure and Mechanical Properties of Thermomechanically Processed β Ti-35Nb-7Zr-5Ta Alloy

Behzad Pourghasemi[1], Vahid Abouei[1,*], Omid Bayat[2], Banafsheh Karbakhsh Ravari[1]

* *vahid.abouei@kiau.ac.ir*

[1] Advanced Materials Engineering Research Center (AMERC) Karaj Branch, Islamic Azad University, Karaj, Iran
[2] Department of Metallurgy and Materials Engineering, Hamedan University of Technology, Hamedan, Iran

Received: November 2021 **Revised: December 2021** **Accepted: February 2022**

DOI: 10.22068/ijmse.2504

Abstract: *It has long been thought-provoking and challenging for researchers to design and produce a special low-modulus β titanium alloy such as Ti□35Nb□7Zr□5Ta, representing optimal mechanical properties needed to simulate bone tissue successfully. To identify the key effects of processing pathways on the development of microstructure, 'Young's modulus, and strength, a nominal Ti-35Nb-7Zr-5Ta alloy was made via casting, hot forging, homogenizing, cold rolling and finally annealing. Results from tensile tests alongside microscopic and XRD analysis confirm the important influence of the processing method on fully β phase microstructure, low elastic modulus, and high strength of the alloy. The specimen with post-deformation annealing at 500°C demonstrated the 'Young's modulus of 49.8 GPa, yield strength of 780 MPa, and ultimate tensile strength of 890 MPa, all of which are incredibly close to that of bone, hence suitable for orthopedic implants. At temperatures above 500°C, a sharp fall was observed in the mechanical properties.*

Keywords: *Ti□35Nb□7Zr□5Ta alloy, Thermomechanical processing, microstructure, Phase transformation, 'Young's modulus.*

1. INTRODUCTION

The need for metal implants that combine high biocompatibility in keeping with desirable mechanical properties, favorable plasticity, and low density resulted in the development of the research in the field of binary and multicomponent nickel-free superelastic alloys based on titanium, such as Ti–Nb, Ti–Nb–Ta, Ti–Nb–Zr [1-4].

The shape-memory effect is observed in the titanium alloys in which the alloying elements prevent the β→ α" phase transformation and play the role of β stabilizers [4-8]. β-type titanium-based alloys containing non-toxic alloying elements such as Nb, Zr, Ta, Sn, Mo, Mn, and Si have been among the most widely used implantable metallic materials [5-9] quaternary alloys such as Ti-Fe-Mn-Zr, Ti-Nb-Ta-Mo, Ti-Nb-Ta-Sn, Ti-Nb-Zr-Mo, Ti-Zr-Mo-Sn along with some quinary alloys like Ti-Nb-Sn-Mo-Zr and Ti-Nb-Zr-Ta-Si have most attention over the past decades.

The main challenge in using Ti base biomaterial alloys is Larger 'Young's moduli compared to human bone in these alloys. In general, a combination of material selection and application of thermomechanically processe should be used to overcome the challenge of high strength with low modulus recently. Ti-Nb-Zr-Ta (TNZT) alloys [3, 9] with the nominal chemical composition of Ti-35Nb-7Zr-5Ta [1, 8, 10-14] have received more attention due to their high strength with low elastic module compared to other Ti-base alloy. Researches show that proper thermomechanically processe can lead to high strength along with low yang modulus inTi-34Nb-7Zr-4.6Ta alloy [10−14].

Polyakov et al. [10] used a severe plastic deformation method to achieve adequate mechanical properties inTi-34Nb-7Zr-4.6Ta alloy. Ferrandini et al. [4] focused on the aging behavior of the Ti-35Nb-7Zr-5Ta and Ti-35Nb-7Ta alloys and concluded that 4 hours aging at 400°C results in the most adequate features for specific purpose. Meng et al. [12] also, have conducted a research on thermomechanical processing of Ti-Nb-Zr alloy through which a good elastic modulus of 48 GPa has eventuated.

This paper considering the high potential of Ti-35Nb-7Zr-5Ta alloy tries to provide a proper thermomechanically process to achieve

[DOI: 10.22068/ijmse.2504]

simultaneous high strength and low elastic modulus

2. EXPERIMENTAL PROCEDURE

2.1. Preparation of the alloy (Thermomechanical processing and heat treatment)

Illustrated in Table 1 are the purity degrees of the elements and the chemical composition of the investigated alloy. The ingot of 300 gr was produced out of bulk elements as raw materials after ultrasonic cleaning in pure ethanol solvent for 30 minutes by vacuum arc re-melting (VAR) furnace and re-melted five times to ensure chemical homogeneity. Afterward, the ingot was hot forged at 1000°C with a cross-section of 8×90 mm^2 to eliminate the coarse dendritic structure. It was then vacuum homogenized by solution annealing heat treatment at 1000°C for 1 hour to resolve micro-segregations and quenched in water to retain a fully β structure at room temperature. To remove surface oxide layers, magnetic field-assisted finishing was used against the specimen surface. Thereafter, 20 cold rolling passes were performed to produce superfine grains and enhance dislocation density with pass reduction of 70%, after which surface cracks would be engendered, culminating in the final thickness of 2 mm. Ultimately, the ingot was cut into four samples for further annealing in order to be recrystallized and decrease defects caused by deformation of the metal at 400°C, 500°C and 600°C for 30 minutes followed by water cooling.

2.2. Mechanical tests and materials characterization

To investigate mechanical properties such as ultimate tensile strength (UTS)(σ_b), yield strength (Y_S)($\sigma_{0.2}$), and elongation (δ), flat bar tension specimens (DIN 10002-1) were cut by wire cut method along the rolling direction from the inner part of the samples due to surface oxidation during annealing. The elastic modulus *E* was calculated according to the slope of the linear portion in the stress-strain curves. Uniaxial tensile testing was performed four times for each dog-bone-shaped specimen (5 mm wide and 0.5 mm thick) based on ASTM E8-M standard utilizing Sntnam 3 tester at a ram speed of 0.005 mm/s in air. The titanium alloy for optical metallography was also polished following a detailed procedure recommended by Buehler Ltd. Using an automatic polisher. The polished samples were etched with a 'Kroll's reagent (10% HNO_3+5% HCl+85% H_2O) for 10 s, and their microstructure were observed by an optical microscope. The microstructures and elemental analysis of the alloy were also examined by a Seron AIS2800C scanning electron microscope (SEM) equipped with an energy dispersive X-ray spectrometer (EDS). The phase constitutions of the specimens were investigated by X-ray diffraction (XRD) analyses, utilized a STOE STADI MP diffractometer over a 2θ range from 20° to 70° at a scanning rate of 0.5°/s with a step size of 0.02° using Copper Kα radiation operating at 40 kV and 250 mA at room temperature. The microstructures of fracture surfaces of the annealed specimens were also evaluated by SEM.

3. RESULTS AND DISCUSSION

3.1. Microstructural feature and phase identification

3.1.1. Thermomechanical processing

To confirm the absence of impurities in the alloy, compositional analysis was examined by EDS, and based on the result, it can be concluded that the alloy is composed of titanium, niobium, zirconium, and tantalum, as observed in Table 1. The SEM micrographs of the as cast (AC), hot forged (HF), solution treated (ST) and cold rolled (CR) Ti□35Nb□7Zr□5Ta alloy are depicted in Fig. 1. AC microstructure is comprised of non-preferred orientation dendrites with coarse morphology due to the segregation of alloying elements during alloy solidification (Fig. 1a).

The HF alloy (Fig. 1b) was obtained after hot forging of the AC specimen replete with band structures in the presence of β-stabilizer elements. It becomes evident that rapid deformation leads to a localized dislocation movement, which is expressed by an increased formation of deformation heterogeneities, namely shear bands [15−18].

Table 1. Chemical composition and elements' purity degrees of the alloy (%).

Elements	Ti	Nb	Zr	Ta
Chemical Composition	52.4	34.7	7.3	5.6

[DOI: 10.22068/ijmse.2504]

Purity Degrees	99.5	99.8	99	99.9

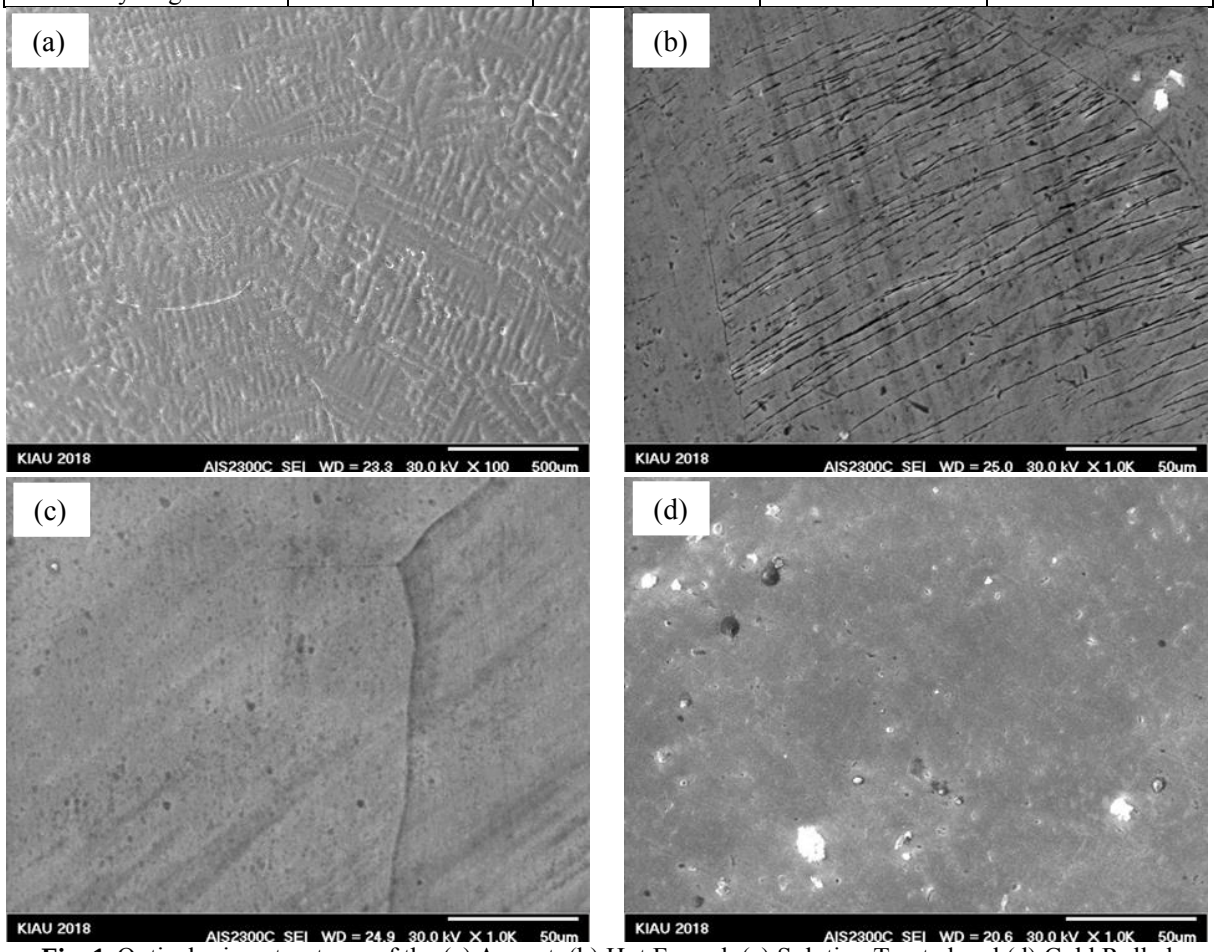

Fig. 1. Optical microstructures of the (a) As cast, (b) Hot Forged, (c) Solution Treated and (d) Cold Rolled alloys.

Solution treatment was done to solve micro-segregations and lower the hardness of the alloy for the further cold working process. After solutionizing, the alloy was composed of large grains of the β phase [13]. ST alloy has a typical equiaxed microstructure, consisting entirely of solely recrystallized β grains (Fig. 1c) due to rapidly cooling from high-temperature β phase. Intense cold rolling has triggered numerous tangles structures [7] with nanosized α precipitated particles in the original β grains (Fig. 1d). XRD diffractograms of ST, CR, 400 and 500°C annealed specimens are shown in Fig. 2. Fig. 2a clearly reveals single-phase BCC β structure diffraction peaks in the as-quenched condition with no alfa precipitated phase and/or isothermal omega phase. As can be seen from Fig. 2b for CR alloy, however, peaks of α phase are obvious due to stress-induced martensitic (SIM) phase transformation, induced during cold rolling of the alloy [15], Wentao et al [16], observed the spherical α and ω precipitate after cold rolling.

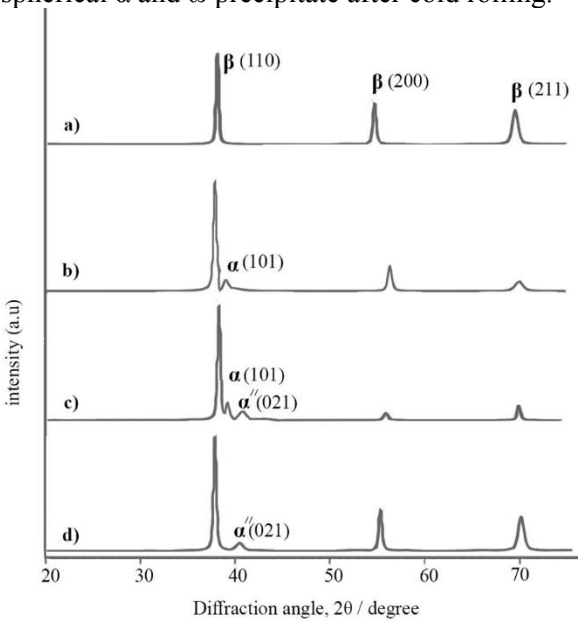

Fig. 2. XRD patterns of the (a) Solution Treated, (b)

[DOI: 10.22068/ijmse.2504]

Cold Rolled, (c) 400°C annealed and 500°C annealed alloys.

Moreover, Xiong et al. [17], approved the formation of needle shape α and ω after cold work, although this phase could not be detected by XRD investigation owing to both its low volume fraction and very fine size of it in the current study. As is evident, after cold rolling, the β phase XRD peaks witnessed a decrease in intensification at both 70° and 56° and also widening behavior in 56°, confirming the substantial increment of crystallographic defects and dislocations, albeit a further hardening of the alloy.

3.1.2. Annealing treatment

Annealed 'specimens' micrographs at 400, 500, and 600°C for 30 minutes are demonstrated in Fig. 3. Annealing heat treatment can bring about recovery, polygonization, and recrystallization of nuclei at the grain boundaries and further formation and growth of them based on temperature and time of the process. The formation of α"" after annealing is also known to be due to releasing residual stress in annealing by Helth et al. [18]. According to XRD profiles of the annealed sample at 400°C (Fig. 2c), the microstructure of this alloy decomposed through α→ α + β, exposing low temperature of annealing to fully resolving the α phase. A needle-like phase can also be seen along the cold rolling direction based on a shear martensitic transformation[19], for which the identification of diffraction patterns confirms the presence of α" martensite. The diffraction lines of the 500°C annealed sample, Fig. 2d, are indexed as the β phases and α" martensite, revealing that α phase was entirely solved at the specified temperature and time. As well as the increase in volume fraction of α" martensite compared with the previous specimen, the width and intensity of the β phase peaks increased markedly as α phase resolved. The result is in accordance with Dubinskiya et al. [20], that report increasing α" formation with increasing annealing Tempereture of Ti–Nb–(Zr, Ta) alloy. In the 600°C annealed state, the α" martensite + β duplex phase structure was identified according to the XRD profile.

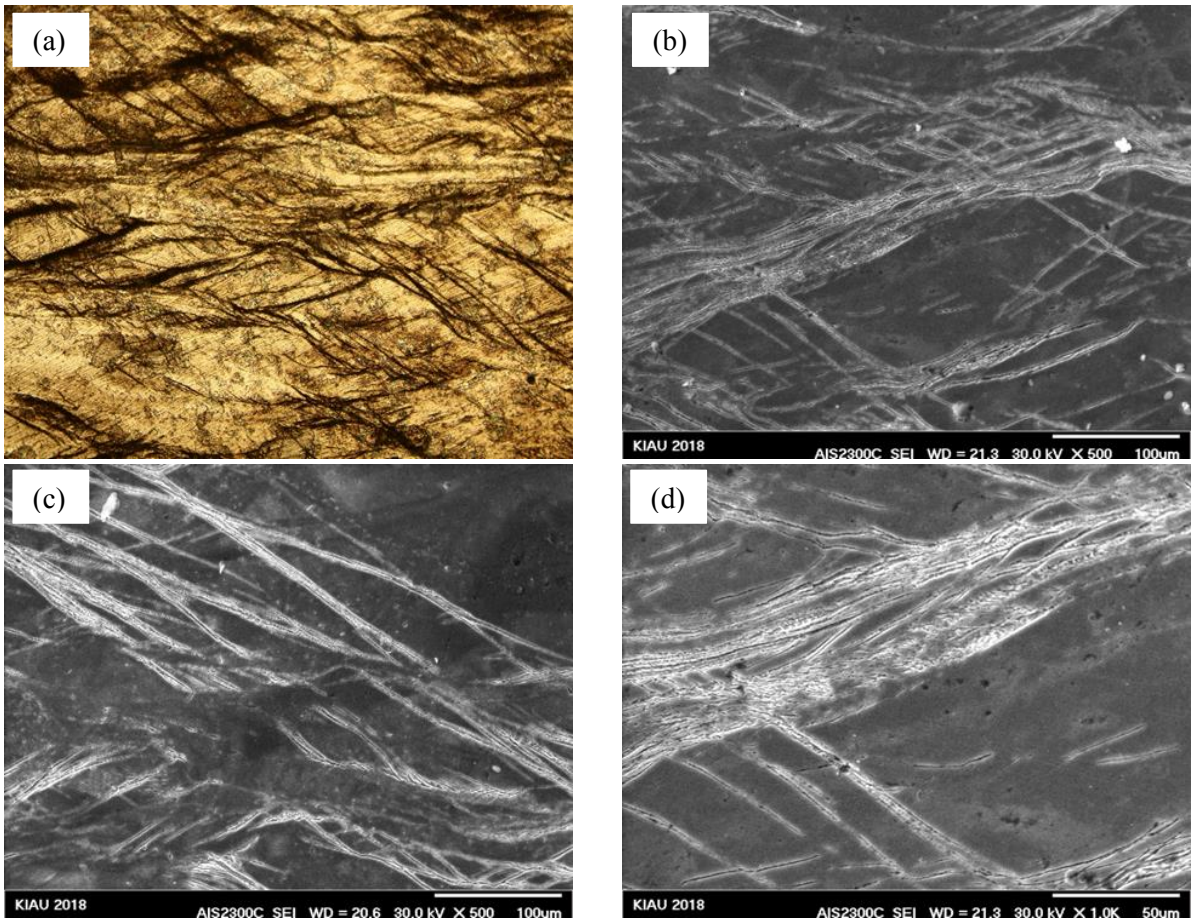

Fig. 3. microstructures of the annealed alloys (a) optical microscopy at 400°C, (b) SEM at 400°C, c) SEM at

[DOI: 10.22068/ijmse.2504]

500°C and (c) SEM at 600°C.

Considering the depletion of the whole tangles and α phases, it could be concluded that the recrystallization phenomenon had thoroughly been taken place at 600°C. As shown by arrows, SEM microstructures in Fig. 3c present the larger size of the α" phase in 600°C annealed alloy compared to 400°C by virtue of the growth of crystal planes or grains after recrystallization.

3.2. Tensile behavior and fracture surfaces

The stress-strain curves of ST, CR, and annealed specimens are reported in Fig. 4, resulting from tensile tests at room temperature. It is seen that all of the alloys exhibit two-stage yielding. Obtained characteristics calculated from the curves are summarized in Table 2. ST alloy has the lowest UTS (710 MPa) with 'Young's modulus (*E*) of 47.3 GPa. Meanwhile, although the UTS of CR specimen has climbed up to 850 MPa its elastic modulus witnessed no significant change (46.2 GPa). After annealing procedure, the 400°C and 500°C annealed samples were in the most hardened state with σ_{max} of 870 and 890 MPa respectively. Changes in mechanical properties due to anteing is in accordance with other researchers reports [21, 22]. Considering simultaneous increase in ultimate tensile strength, the α" martensite might be moderately precipitated with rising annealing temperature [14], as it is distinguished from the XRD pattern It should also be noted that the relative intensity of these β and α" peaks changed due to different annealing temperature. In both cases XRD diffractograms confirm phase constitutions as single β phase with imposed α" martensite, deplete with α phase for annealing at temperatures higher than 400°C.

SEM fracture micrographs of the 400°C and 500°C annealed specimens are depicted in Fig. 5 after tensile test.

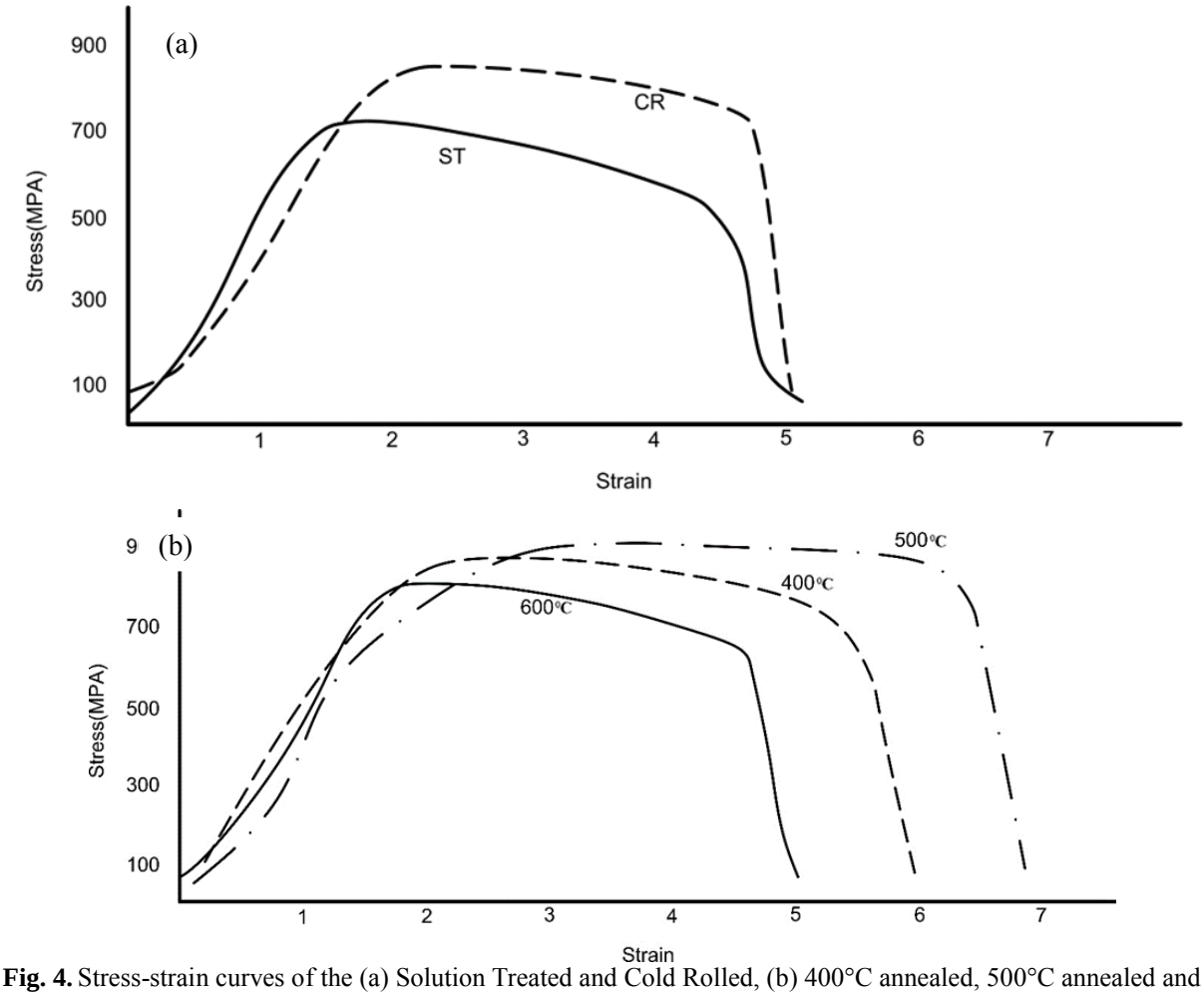

Fig. 4. Stress-strain curves of the (a) Solution Treated and Cold Rolled, (b) 400°C annealed, 500°C annealed and

[DOI: 10.22068/ijmse.2504]

600°C annealed alloys.

Table 2. 'Young's modulus *E*, ultimate tensile strength UTS, true yield strength YS and relative elongation to failure (δ) for ST, CR and annealed samples.

	***E*, GPa**	**UTS, MPa**	**YS, MPa**	**δ%**
ST	47.3	710	610	5.3
CR	46.2	850	740	5.2
400°C	47.9	870	760	6
500°C	49.8	890	780	7
600°C	46.5	790	730	5.1

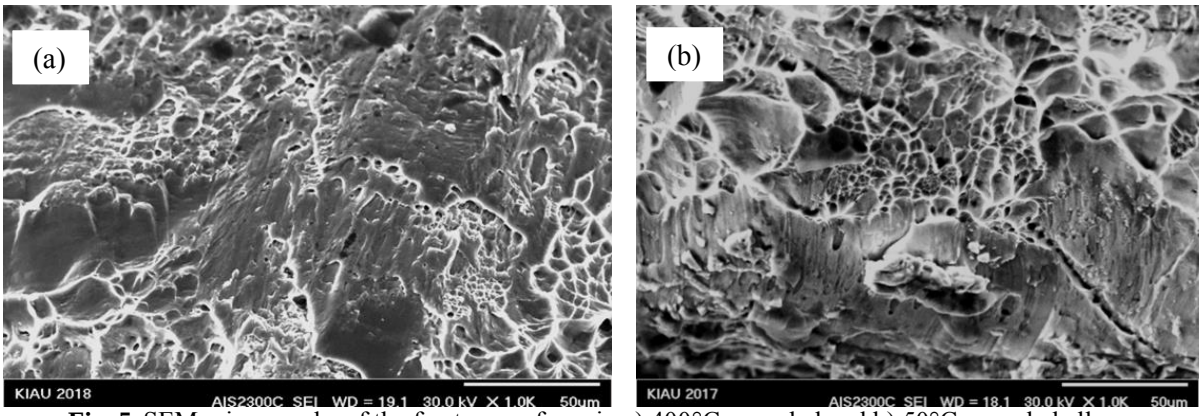

Fig. 5. SEM micrographs of the fracture surfaces in a) 400°C annealed and b) 50°C annealed alloys.

The ductile mechanism of the fractured surfaces is confirmed due to the presence of dimples for both annealed alloys. It can additionally be seen cleavages combined with ductile dimples in 400°C annealed sample. No brittle intergranular failure, however, was observed in any of the fracture surfaces. This also indicates that the annealed samples have large plastic deformation ability.

As a result, satisfying combination of low 'Young's modulus, high tensile strength, and proper ductility makes this titanium alloy (500°C annealed sample) an excellent candidate for biomedical applications. This could be acceptable and have been reported by other researchers [23].

4. CONCLUSIONS

The combination of thermomechanical processing, comprising of hot forging, solution treatment, and cold rolling coupled with-annealing treatment,was applied to Ti35Nb7Zr5Ta biomedical alloy, aiming to develop static tensile properties of this alloy. Below-mentioned conclusions are the primary outcomes of the research.

a) As a result of grain structure refinement, the ultimate tensile strength increased from 710 regarding ST alloy to 890 MPa for 500°C annealed specimen, and the relative elongation changed significantly (from 5.3 to 7%).
b) Annealed at 500°C results in a complete solution of α phase in the parent β phase in line with the existence of α" martensite.
c) 'Young's moduli of all the alloys are within the range of 46.22 to 49.8 GPa. The differences of 'Young's moduli are not noticeable; however, the ultimate tensile strength of the specimens varies significantly.
d) The 500°C Ti35Nb7Zr5Ta annealed alloy shows an excellent combination of low 'Young's modulus (49.8 GPa) and high ultimate tensile strength (890 MPa) of which are close to the human bone as is expected.

REFERENCES

[1] Afonso, C.R., Ferrandini, P.L., Ramirez,

[DOI: 10.22068/ijmse.2504]

A.J., Caram, R., "High resolution transmission electron microscopy study of the hardening mechanism through phase separation in a beta-Ti-35Nb-7Zr-5Ta alloy for implant applications". Acta Biomaterialia. 2010, 6(4), 1625-1629.

[2] Banerjee, P., Chiranjit, R., Mohamed, A., Amit, R., Soumya, B., Somnath, B., "Probing Nanoscale Phase Separation at Atomic Resolution within β-Type Ti–Mn Alloy: A Potential Candidate for Biomedical Implants", ACS Biomat. Sci. & Eng., 2019, 5 (10), 5005-5014.

[3] Cho, K., Niinomi, M., Nakai, M., Hieda, J., Kanekiyo, R., "Improvement of Tensile and Fatigue Properties of beta-Titanium Alloy while Maintaining Low Young's Modulus through Grain Refinement and Oxygen Addition". Mat. Trans., 2013, 54, 2000-2006.

[4] Ferrandini, P. L., Cardoso, F. F., Souza, S. A., Afonso, C. R., Caram, R., "Aging response of the Ti-35Nb-7Zr-5Ta and Ti-35Nb-7Ta alloys". J. All. and Comp., 2007, 433(1-2), 207-210.

[5] Fu J., Kim H.Y., Miyazaki, S., "Effect of annealing temperature on microstructure and superelastic properties of a Ti-18Zr-4.5Nb-3Sn-2Mo alloy." J.Mech. Behavior of Biom. Mat., 2017, 65, 716-723.

[6] Jiang, B., Qing, W., Donghui, W., Fen, X., Guoqing, C., Chuang, D., Lixian, S., Peter, K. L., "Effects of Nb and Zr on structural stabilities of Ti-Mo-Sn-based alloys with low modulus", Mat. Sci.and Eng. A, 2017, 687, 1-7.

[7] Lan, C., Yu, W., Lili, G., Feng, C., "Effects of cold rolling on microstructure, texture evolution and mechanical properties of Ti-32.5Nb-6.8Zr-2.7Sn-0.3O alloy for biomedical applications", Mat. Sci. and Eng. A, 2017, 690, 170-176.

[8] Li, Y.H., Yang, C., Wang, F., Zhao, H.D., Qu, SG, Li, X.Q., Zhang, W.W., Li, YY, ""Biomedical TiNbZrTaSi alloys designed by d-electron alloy design theory". Mat. & Design, 2015, 85, 7-13.

[9] Yang, Y., Li, G.P., Cheng, G. Li, Y., Yang, K", Multiple deformation mechanisms of Ti–22.4Nb–0.73Ta–2.0Zr–1.34O alloy"." App. Phy. Lett. 2009, 94, 10.1063-1.3078521.

[10] Polyakov, A., Semenova, I., Ivanov, E., Valiev, R., "Ultra-fine grained β-type TNZT ELI alloy with high strength and low elastic modulus". IOP Conference Series: Mater. Sci. Eng., 461. 012077. 10.1088/1757-899X/461/1/012077.

[11] Plaine, A.H., Silva, M.R., Bolfarini, C., "Effect of Thermo-Mechanical Treatments on the Microstructure and Mechanical Properties of the Metastable β-type Ti-35Nb-7Zr-5Ta Alloy". Mat. Rese., 2019, 22, https://doi.org/10.1590/1980-5373-MR-2018-0462.

[12] Meng, Q., Shun, G., Qing, L., Liang, H., Xinqing, Z., "A β-type TiNbZr alloy with low modulus and high strength for biomedical applications", Prog. Natu. Sci. Materials International, 2014, 24, 157-162.

[13] Ozan, S., Lin, J., Li, Y., Zhang, Y., Munir, K., Jiang, H., Wen, C., "Deformation mechanism and mechanical properties of a thermomechanically processed β Ti-28Nb-35.4Zr alloy". J. Mech. Behav. Biomed Mater., 2018, 78, 224-234.

[14] Sun, Y., Yang, S., Jianlin, Z., Shengqun, W., Zhongli, G., "Biocompatibility evaluation of novel β-type titanium alloy $(Ti–35Nb–7Zr–5Ta)_{98}Si_2$ in vitro". RSC Advances, 2015, 5(123), 101794-101801.

[15] Zhang, D.C., Tan, C.G., Tang, D.M., Zhang, Y., Lin, J.G., Wen, C.E., "Effect of thermomechanical treatment on the superelasticity of Ti-7.5Nb-4Mo-2Sn biomedical alloy". Mat. Sci. Eng. C Mater Biol Appl., 2014, 44, 76-86.

[16] Chengyang, X., et al., "Phase transformations and microstructural evolution in Ti-19.5Zr-10Nb0.5Fe shape memory alloys", Materials Characterization, 2017, 133, 156-164.

[17] Wentao, Q., Xuguang, S., Bifei, Y., Chengyang, X., Yan, L., Yongsheng, N., ""Phase transformation and microstructure evolution of the deformed Ti-30Zr-5Nb shape memory alloy"," Mater Charact., 2017, 126, 81-85.

[18] Helth, A., Pilz, S., Kirsten, T., Giebeler, L., Freudenberger, J., Calin, M., Eckert, J., Gebert, A., "Effect of thermomechanical processing on the mechanical biofunctionality of a low modulus Ti-40Nb

[DOI: 10.22068/ijmse.2504]

alloy", J Mech Behav Biomed Mater., 2016, (65), 137-150.

[19] Tang, X., Ahmed, T., Rack, H.J., "Phase transformations in Ti-Nb-Ta and Ti-Nb-Ta-Zr alloys". J.Mat. Sci., 2000, 35, 1805–1811.

[20] Dubinskiy, S. M., Prokoshkin, S. D., Brailovski, V., Inaekyan, K., Korotitskiy, A.V., Filonov, M.R., Petrzhik, M.I., "Structure formation during thermomechanical processing of Ti- Nb-(Zr, Ta) alloys and the manifestation of the shape-memory effect", Phys. Met. Metallogr., 2011, 112(5), 529–542.

[21] Brailovski, V., Prokoshkin, S.D., Gauthier, M., Inaekyan, K., Dubinskiy, S.M., Petrzhik, M.I., Filonov, M.R., "Bulk and porous metastable beta Ti–Nb–Zr (Ta) alloys for biomedical applications", Mat. Sci. and Eng., 2011, C 31(3), 643–657.

[22] Kim, H.Y., J.F., Tobe, H., Kim, J.I., Miyazaki, S., "Crystal structure, transformation strain, and superelastic property of Ti–Nb–Zr and Ti–Nb–Ta alloys", Shape Mem Superelasticity, 2015, 1, 107–116.

[23] Sheremetyev, V., "Structure and functional properties of metastable beta Ti-18Zr-14Nb (at. %) alloy for biomedical applications subjected to radial shear rolling and thermomechanical treatment", J. All. and Comp., 2018, 737, 678-683.

[DOI: 10.22068/ijmse.2504]